

## Modeling, Model Verification, and Defect Formation in Iron Castings

Wanliang Sun, Preston Scarber, Hanjun Li, and Charles E. Bates  
University of Alabama at Birmingham, Birmingham, Alabama

### ABSTRACT

Experiments are being conducted in a real-time x-ray system to examine the flow of iron into molds and how the flow characteristics affect defect formation. The purpose is to 1) determine the effects of various gating systems on turbulence and oxide formation, 2) examine the effects of core processing variables on porosity in castings, and 3) extend the data using models for castings that cannot easily be examined in an x-ray system.

Mold-metal interface reactions and gas evolution have been observed during and after the metal pouring. The fill behavior and mold-metal reactions significantly affect casting quality. Gas holes and gas pores were found in castings poured turbulently and in castings poured with cores where core permeability was inadequate to allow all gasses to escape. Mold coatings affect gas evolution and the surface quality of castings made in resin bonded molds. Surface defect locations were related to gas bubbling during and after mold filling. Gas pores were also produced by pyrolysis of volatiles in the coating and from the decomposition products of core binders. When volatiles cannot escape through the sand, gas bubbles through the casting and produces gas holes. Cores with inadequate permeability also caused gas to bubble through the metal to produce defects.

This research is being conducted to develop procedures for pouring iron inside a vault to visualize and then minimize defect formation, and then extend the technology to castings that cannot easily be poured in the x-ray system through the use of models. The ultimate goal is to develop procedures for pouring and gating that will reduce foundry scrap to negligible values.

### INTRODUCTION

Metal filling of mold cavities has historically been studied using several techniques: 1) removing the mold cope and watching flow through a quartz plate, 2) using real-time x-rays to penetrate the mold and observe metal front movement, 3) using water simulations (Perkins and Bain, 1965; Nguyen and Carring, 1986; Xue et al, 1993), 4) using computer modeling, and 5) embedding position probes to follow metal fronts during filling. However, real-time x-ray systems provide the best method for observing mold filling with minimal external interference (Campbell and Koster, 1994).

Fry (1944) was perhaps the first to use a real-time x-ray system to observe metal fill behavior. Others, including St. John *et al.* (1980), Sirrell and Campbell (1995), Barkhudarov and Williams (1995), Ruiz and Khandia (1995), Sirrell *et al.* (1996), Yang and Campbell (1998), Jolly *et al.* (1998) and Schuhmann, Dale, *et al.* (2000) have used the real-time x-ray observations to compare fill behavior to simulations.

X-rays are also used to relate metal filling to casting quality. Ashton and Buhe (1973) used this technique to study the effects of gating system design on defect formation. Stegemann, Reimche, and Schmidbauer (1992) examined defect formation in light metal castings. Lee *et al.* (1995, 1997, 1997) and Atwood *et al.* (1999, 2000) constructed an X-ray Temperature Gradient Stage (XTGS) to watch hydrogen porosity develop in aluminum during controlled directional solidification. Sirrell and Campbell (1997) examined the effect of filtration on defect formation, and Rezvani and Campbell (1999) related x-ray observations made during filling to the strength and reliability of cast aluminum. Castings poured with a minimum of turbulence had higher mechanical properties. X-ray technology has also been used to observe metal filling in permanent molds (Schuhmann, Dale, *et al.*, 2000) and lost foam molds (Sun, Littleton, Bates, 2002).

By contrast, fewer studies have been conducted using real-time x-ray to study gray iron mold filling, probably because of the higher pouring temperature and greater difficulty of penetrating the metal. Also, relatively few studies have been conducted focusing on gas porosity formation.

**EXPERIMENTAL PROCEDURES**

A 320 kV real-time x-ray system was used in the current study to observe metal filling, mold-metal reactions, and the defects formed in gray and ductile iron castings. Some molds were coated with commercial mold washes to create a variety of conditions inside the mold cavity. Other molds had cores inserted to observe gas evolution during and after pouring. The effects of the mold conditions, metal fill behavior, and the mold-metal interface reactions were recorded during pouring and subsequently examined to determine the phenomena responsible for defect formation.

**Uncored Plate Mold**

The molds used in this study were produced using phenolic urethane (PUCB), toluene sulphonic acid catalyzed phenolic (TSAP) resin, and Alpha Set resin binders. Most cores examined to date have been made by the shell (Kroning) process. The sand used has been as coarse as GFN-25 and as fine as GFN-80.

The appearance and dimensions of the uncored plate mold are illustrated in Figure 1. The casting cavity was a plate with dimensions of 102mm × 102mm × 13mm (4in × 4in × 0.5in). The mold had a tapered sprue with a built-in pouring basin on top of the sprue. The gating system was choked at the ingate, making the gating system a pressurized system.

Selected molds were coated with a commercial alcohol-based wash to create various mold permeability conditions. In all cases, the coatings were sprayed on and the alcohol burned off. Thicker coatings producing lower mold permeability were obtained by applying more than one coating. The alcohol in each layer was burned off prior to applying the next layer. Coating thicknesses were measured using a thickness gauge and the value recorded.

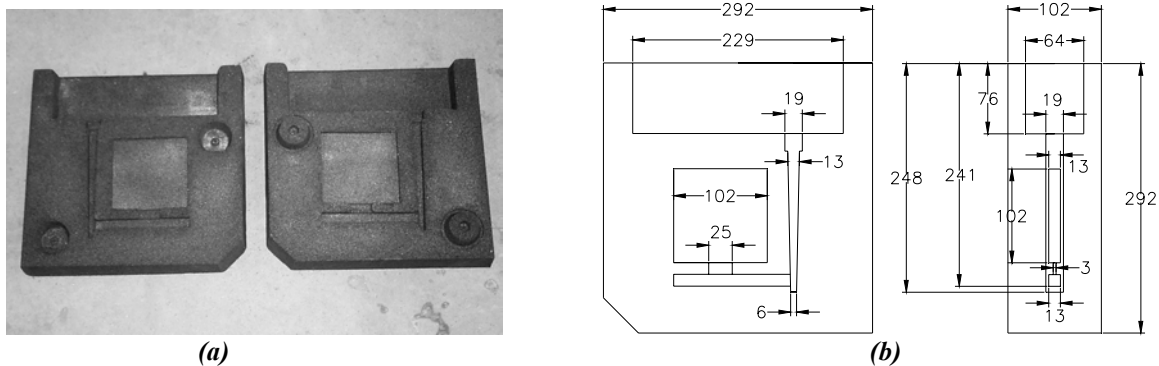


**Fig. 1. (a) Macrograph of experimental plate mold. (b) Dimensions of the plate mold.**

**Cored Plate Mold**

The plate mold containing a core is shown in Figure 2 with dimensions in millimeters. The sprue was slightly tapered and the pouring basin on top of the sprue was on the opposite half of the mold. The gating system was choked at the ingates, which resulted in a slightly pressurized system.

The cores used to date were made using the shell process. The cores were stored in a dry environment and were individually wrapped to avoid contamination or scratching of the surfaces.

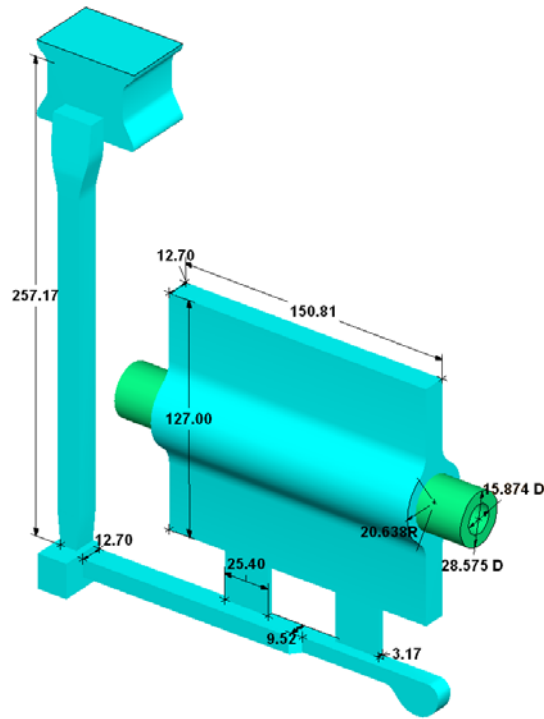


**Fig. 2. Solid model of the cored plate casting used in the real-time x-ray observations. All dimensions are in millimeters.**

Vibration Dampener Mold

A dimensioned solid model of the vibration dampener casting is shown in Figure 3. The sprue for this casting was untapered and the dimensions of all flow channels increased as liquid approached the casting cavity, resulting in an unpressurized gating system. A stoppered basin was placed above the sprue to produce consistent pouring conditions. .

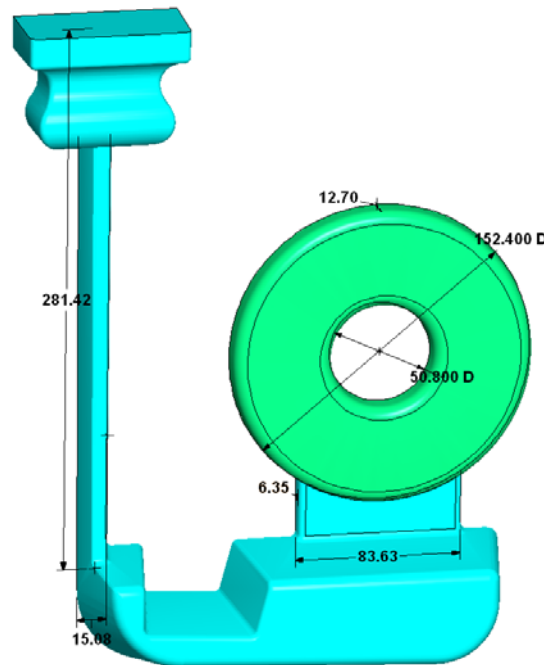


**Fig. 3. Solid model of the vibration dampener used in the real-time x-ray observations and computer simulations. All dimensions are in millimeters.**

## 2003 Keith Millis Symposium on Ductile Cast Iron

### MELTING AND POURING

Castings were poured with both gray iron and ductile iron. The gray iron was a class 30 material containing nominally 3.4% C, 2.2% Si, 0.60% Mn, and 0.08% S. The iron was inoculated with a 0.2% addition of 75% ferrosilicon during tapping from the melting furnace and poured at a temperature of approximately 2500° F.

Ductile iron castings contained approximately 3.65% C, 2.5% Si, 0.40% Mn, and 0.035% Mg. The base iron was melted using steel scrap, silicon carbide, crystalline graphite, and ferro-manganese. The irons were inoculated with a 0.5% addition of 75% inoculating grade ferrosilicon during tapping from the furnace. All iron was melted in a 45kg (100lb) induction furnace, tapped, and poured in the range of 2500°F -2600°F (1370°C -1425°C).

### X-RAY SYSTEMS

There are two x-ray units inside the vault. One system, a 320 kV tube having a focal spot size of 0.8mm × 0.8mm, is used to observe metal flow into molds. The x-rays are imaged on a 9" diameter tri-field image intensifier and photographed using a Sony XC75CCD camera. A microprocessor console integrates the operation of this unit so that images are captured correctly.

The second unit consists of a 160 kV micro-focus x-ray tube, with a focal spot ranging in size from 5 to 200 microns depending on the current applied, and an A-SI (amorphous silicon) digital detector having an active area of 203 × 254mm and 1997 × 2592 (3.1million) pixels. Each pixel in the digital detector has a 12-bit gray scale density resolution when maximum resolution is desired. The detector can provide 4096 shades of gray at a frame speed of 7 frames per second. At a frame rate of 30 frames per second, there are 256 shades of gray. Both x-ray systems can be used for real-time and static examinations of cast parts, although the micro-focus unit does not have the penetrating ability of the 320 kV tube. In this study, the 320kV system was used for real time observations, and the 160kV digital system was used to evaluate internal casting quality.



*Fig. 4. (a) Overview the x-ray system. (b) Close-up view of mold and pouring cart.*

A view of the x-ray vault with the door open is illustrated in Figure 4 (a), and a mold and the pouring cart is shown in Figure 4(b). Although either horizontally split or vertically split molds can be poured in the x-ray vault, the molds used in this study were poured with a vertical parting line. Mold halves are assembled outside the x-ray vault, and the halves locked together with wood plates and threaded rod. The support plates allow green sand as well as no-bake moles to be poured. There is a spacer between the mold and the support plate to allow gas to freely exit from the back of the mold. Each mold is placed inside the x-ray vault, a cart holding a ladle of liquid metal is positioned in the vault using steel tracks, and the metal remotely poured from the pouring cart into the mold. The pouring cart can be raised or lowered to accommodate various mold sizes. The pouring rate is controlled manually by watching output from two cameras in the vault. X-rays pass through the mold and are projected onto a cesium-iodide (CsI) fluoroscopic screen, photographed at 30 frames per second using a CCD camera, and recorded on a VCR. The video images are later converted to digital files for image processing.

Velocity profiles were processed to obtain isochronal metal front profile maps. Changes in the metal front profile could be clearly seen, and instantaneous metal fill velocities calculated using time steps of 0.1 sec. The front profile maps were used to compare the metal filling using different mold conditions.

Fill behavior has been compared to computer models in some cases to verify and / or adjust the models. This allows models to be used outside the range of mold sizes that can be poured and viewed in the vault.

## RESULTS AND DISCUSSION

### MOLD COATING EFFECTS ON FILLING

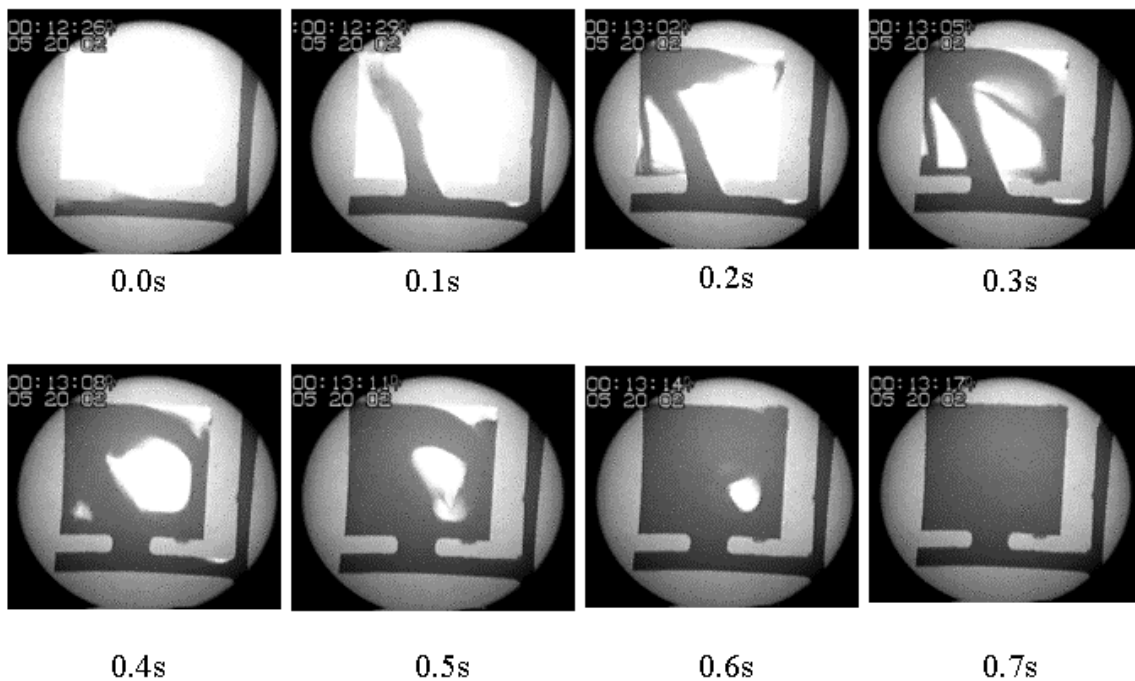


*Fig. 5. Video stills of the metal filling of the mold without coating.*

Several video “frames” at different times during filling are illustrated in Figure 5. The mold wall has its maximum permeability when no coating is used, and the metal entered the mold cavity at about 90 cm/s (35in/s). After the molten metal hit the mold wall, it splashed, swirled, and entrapped air. A low pressure region near the junction of the sprue with the horizontal runner was found to persist over about 75 % of the pouring event. The metal filling was so turbulent that it was difficult to make an isochronal metal front map.

Coating the mold reduced the mold permeability and metal flow rate into the mold. Isochronal front maps at 0.1 second after the start of pouring of molds with no coating, one layer, two layers, and three layers of coating are illustrated in Figure 6. These maps were obtained by tracing the metal front at 0.1 second time intervals. The metal fill rate became slower and smoother when thicker coatings were applied. The increased coating thickness had two effects: (1) it reduced the permeability of the mold and (2) produced more gas as the volatiles in the coating evolved. These factors increased the gas backpressure and slowed the fill rate.

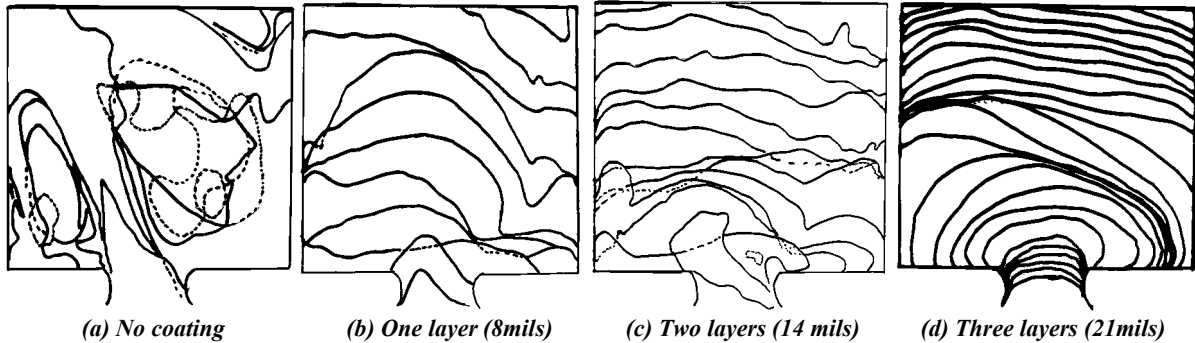


*Fig. 6. Isochronal metal front profile map of the metal filling in sand molds coated at different thickness. The maps were obtained by tracing the metal flow at every 0.1s.*

## MOLD - METAL INTERACTIONS

### Cold Shot

The high velocity metal stream caused splashing and metal shot formation when the mold was poured without any coating. The shot oxidized and then froze when it hit a cold portion of the mold. Cold shot on the mold wall is illustrated in Figure 7(b). The cold shot may be flushed back into the casting by the whirling metal flow to produce internal anomalies.

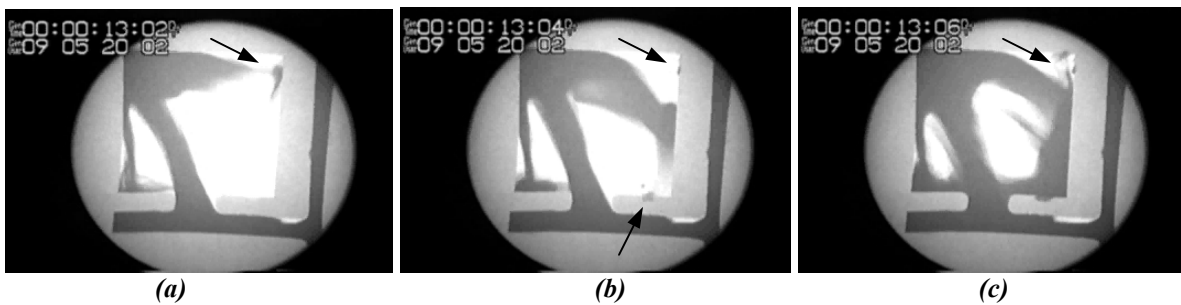


*Fig. 7. Cold shot caused by splashing during mold filling.*

### Air Entrapment

Some air entrapment was also observed as metal was poured into uncoated molds. The whirling metal illustrated in Figure 8(a) entrapped some air. Most of the nitrogen probably escaped, but the oxygen reacted with iron to produce reoxidation products that can be found both on the surface and on the interior of castings.

Air entrapment was also observed in the metal filling of coated molds. Mold filling was turbulent near the ingate, and air entrapment occurred as illustrated in Figure 8(b). Although the entrained air later disappeared, iron and silicon oxides were formed which affect surface quality and machinability.

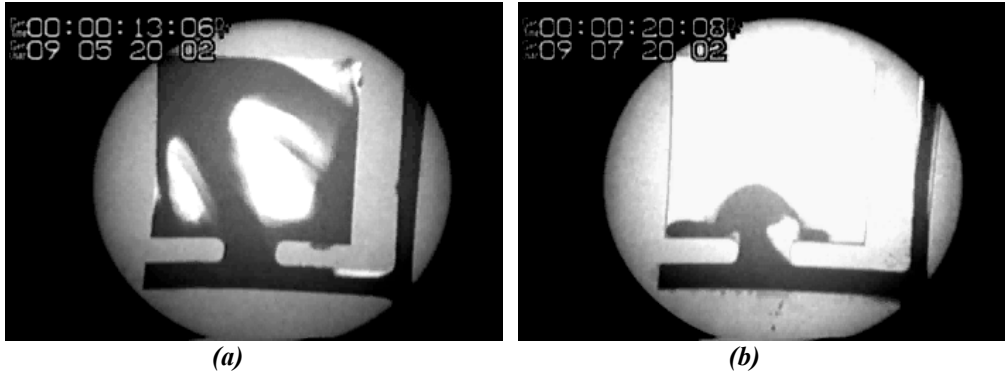


*Fig. 8. (a) Metal filling an uncoated mold; (b) Metal filling a coated mold*

### Plate Casting Quality

Mold reactions affect the surface and internal casting quality. The surface quality was described using macrographs of the as-cast surfaces, and the internal casting quality was evaluated using digital x-rays. The advantage of digital macrographs and x-rays is that they are easily transported for viewing by other investigators, and analysis can be conducted with image analysis software.

The appearance of a casting poured in an uncoated mold was shown in Figure 9(a). The surface of the casting was rough and burned-on sand was present over the surface. A gas hole marked by "A" is illustrated in Figure 9(a). This gas hole was also seen in the digital x-ray in Figure 9(b). More pores are visible in the x-ray which indicates do not extend to the casting surface.

The surface of a casting poured in a coated mold is illustrated in Figure 10. The coating improved the casting surface finish as illustrated in Figure 10(a) and (b) and reduced the number of internal defects compared to the uncoated mold (see Figure 9 (b)). Some gas porosity is still present, indicating that other factors such as the gating system must be changed to produce a quality casting.

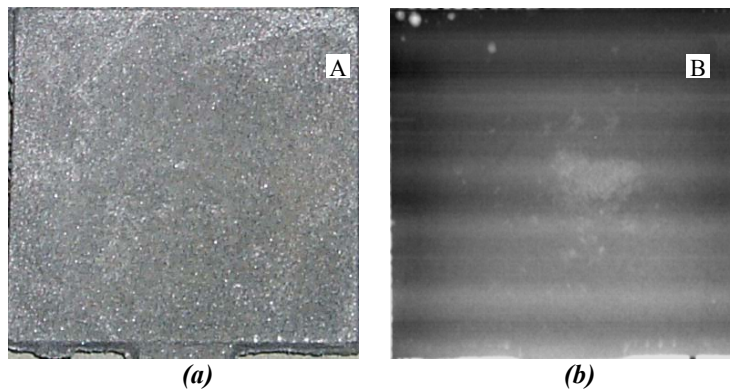


*Fig. 9. (a) Photograph and (b) Digital X-Ray of casting.*

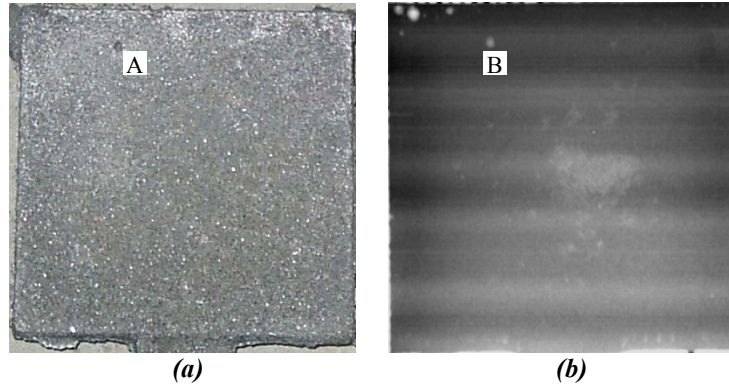


Fig 10. (a) Photograph and (b) digital x-ray of a casting with mold wash

Core Gas

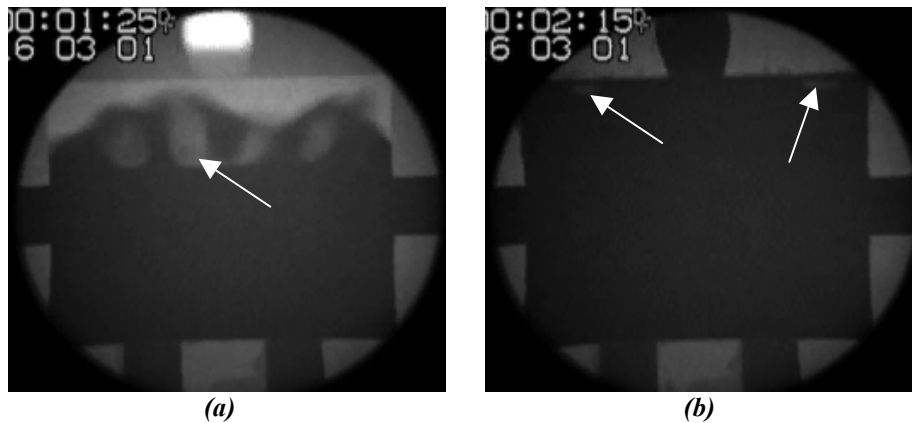


Fig. 11. Mold gas observed in the metal filling. (a) Gas Generation; (b) Gas Entrapped in the metal.

Core gas produced during filling a cored plate mold with ductile iron is illustrated in Figure 11. As the binder decomposed, the gas will either exit through the core or bubble through the metal to produce porosity. This gas bubble damage can be aggravated by residual volatiles in the mold coating.

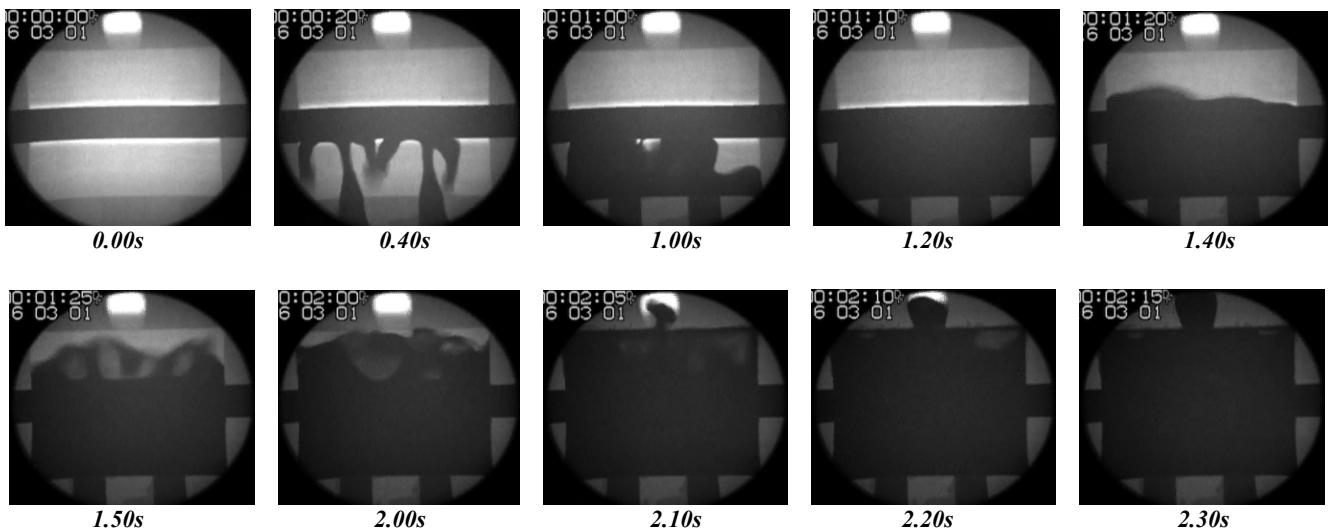
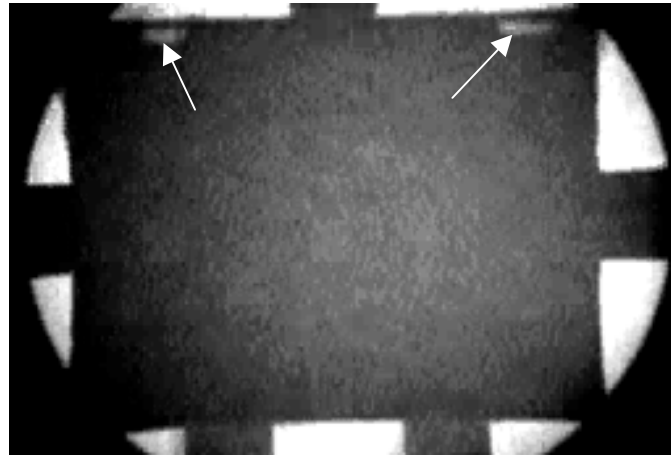


Fig. 12. Observations of the mold gas after the metal filling.

Video stills shown in Figure 12 illustrate gas bubbling through the casting. Gas bubbles were observed at 1.40, 1.50, 2.00, and 2.10 seconds into mold fill. The image in Figure 13 was obtained after solidification. The gas is visible at the top edge of the casting just below the metal surface.



*Fig. 13. Subsurface Gas Porosity in Ductile Iron Casting.*

#### Modeling and Model Verification Using a Vibration Dampener Casting

Slow-motion video from real-time x-ray observations can be used to verify the accuracy of casting simulations. Simulation boundary conditions were set to match the experimental procedure as closely as possible while keeping the number of computational cells at a minimum. Real-time x-ray images and simulation surface plots are shown in Figure 14. Many of the fluid contours in the x-ray images are mimicked almost exactly by the simulations. After 2.20s of mold fill, the two liquid metal fronts impinge and form a liquid prominence; this behavior is shown in both the simulation and the x-ray frames illustrated in Figure 14.

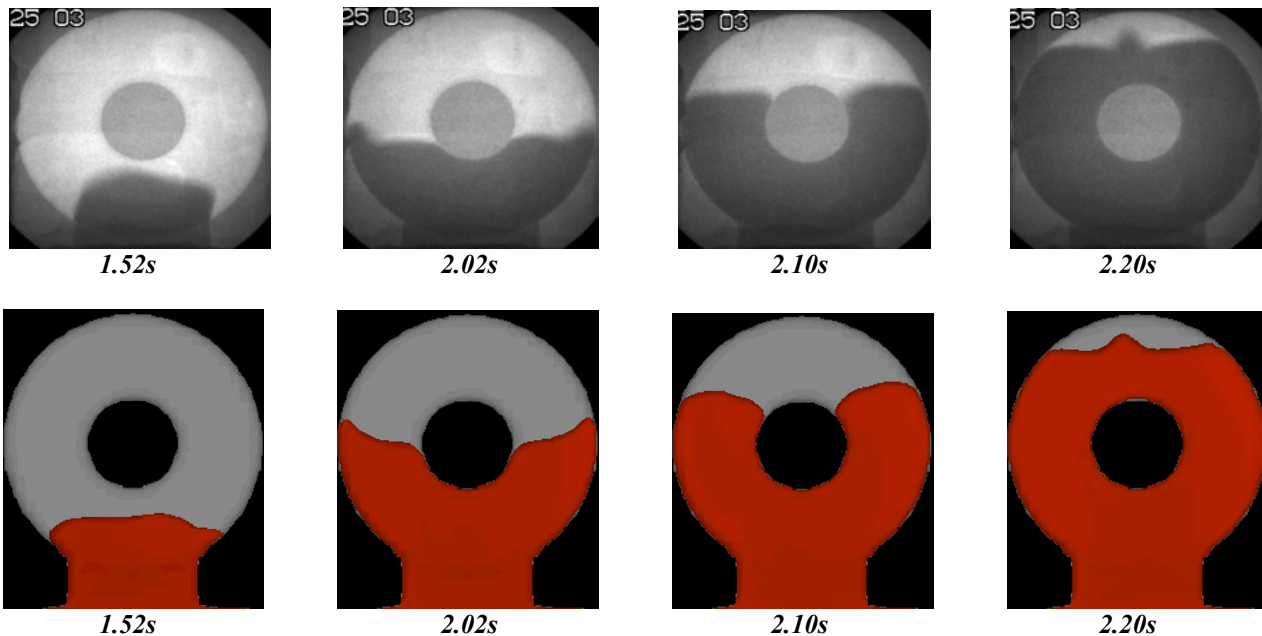


*Fig. 14. Real-time x-ray and simulation fluid contours of mold fill in the vibration dampener casting.*

Extending Models to More Complex Castings

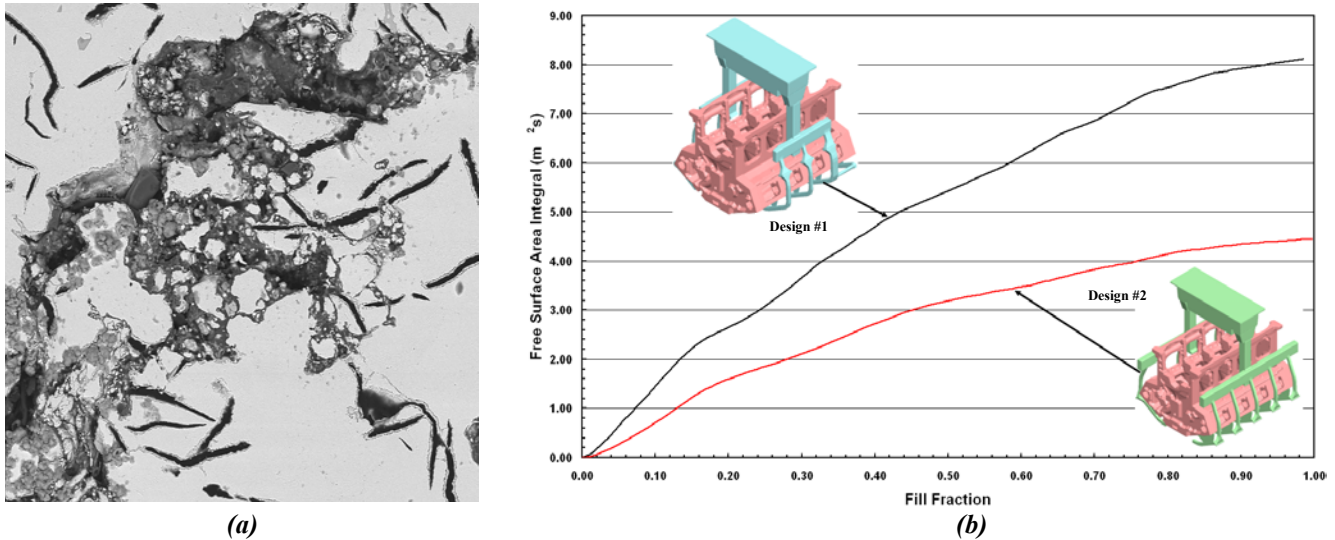


**Figure 15. (a) SEM backscatter electron image of a reoxidation defect in gray iron – 250x magnification. (b) Plot of liquid surface area vs. fill fraction for an engine block with two different gating systems.**

Research to determine riser size and placement has been underway for at least a century, and within the last 20 years, rising principles have been incorporated into all commercial computer codes. Much less has been done on the mold filling process. Oxidation during pouring is responsible for much of the dross and surface defects on both gray and ductile iron castings. A typical dross defect in a gray iron casting found during machining is illustrated in Figure 15a, and those in ductile iron are similar.

Filling of molds made on a Hunter or small Disa can be viewed directly with the real time x-ray system. But the system is more valuable when used to compare fill patterns with simulation results and then extend use simulations to predict turbulence in castings too large or complex to view with an x-ray system.

The time and area of metal contact with air during pouring and mold filling largely controls surface and subsurface inclusion formation. Data and theories were incorporated in a simulation of an eight cylinder engine block, and the results are illustrated in Figure 15b. Several simulations were run and the original gating system redesigned to reduce metal turbulence and splashing. Initially, the metal contact with air was over 8 m<sup>2</sup> sec. Gate modification reduced exposure to 4 m<sup>2</sup> sec. The oxide defect scrap rate on the block with the original production gating system was about 5%. When gate changes were incorporated to reduce turbulence and surface contact with air, the oxide defect rate dropped to 0% and has been at this value for almost a year.

**SUMMARY**

This study was conducted to explore the use of real time x-rays for observing defect formation during filling molds with iron. Sand molds bonded with various binders were coated with various amounts of an alcohol-based mold wash. No variations were made in the gating system.

Procedures were developed for pouring iron and observing mold filling using high-energy x-rays. The fill patterns were recorded and later analyzed to study the formation of surface and internal casting defects. The following observations were made:

## 2003 Keith Millis Symposium on Ductile Cast Iron

1. Mold coating plays an important role in mold filling. In general, the coating has lower permeability than the mold; and the reduced permeability, in the absence of a vent, reduced the metal entry velocity and produced a much smoother cavity fill pattern.
2. Metal-mold interface reactions and mold gas formation were observed during and after the metal filling of molds having a thick layer of mold wash. The residual volatiles in the mold wash were evolved as the wash was heated by the molten metal. Gas-induced gaps and bubbling through the casting were observed during and after the cavity was filled.
3. The volume of gas produced by cores during mold fill was large enough to cause subsurface gas defects in every casting examined in this study. This damage occurs in every cored casting when consideration of core gas movement is not considered.
4. Simulations of castings observed with the x-ray system showed high accuracy with experimental results. Analysis of simulation results revealed that high liquid surface area correlated well with increased air entrainment.
5. Simulations of the free surface behavior during mold fill of a large casting showed that a change in gating system would reduce liquid surface area by more than 50% during mold fill. Experimental results proved the validity of simulations, resulting in a complete elimination of scrapped castings.

## REFERENCES

- Ashton, M.C., Buhr, R.K., Internal Report PM-1-73-5, Canada Department of Energy, Mines and Resources, Mines Branch, Ottawa, (1973)
- Atwood, R.C., Sridhar, S., Zhang, W. and Lee, P.D., Diffusion-controlled Growth of Hydrogen Pores in Aluminum -silicon Castings: in situ Observation and Modeling. *Acta Materialia*, Vol.48, Jan. 24, 2000:405-417.
- Atwood, R.C., Sridhar, S., Zhang, W. and Lee, P.D.. Equations for Nucleation of Hydrogen Gas Pores during Solidification of Aluminum Seven Weight Percent Silicon Alloy. *Scripta Materials* Vol. 41, No.12, 1999:1255-1259
- Barkhudarov, M., Williams, K., Simulation of surface turbulence fluid phenomena during mold filling. *AFS Transactions*, 95-90, pp 669-674 (1995).
- Campbell, T. A., Koster, J.N., Visualization of liquid -solid interface morphologies in gallium subject to natural convection. *Journal of Crystal Growth*, Vol 140, 1994:414-425
- Davis, K. G., Magny, J.G., Trapping slag and nonmetal material in gating systems for cast iron and steel," *AFS Transactions*, Vol 85, pp 227-236(1977)
- Fry, S.L., Preliminary Investigation of Metal Pouring by Cine Radiography, *Proceedings of the Institute of British Foundrymen*, Vol. 39,1944-45, pp 44-54 (1944)
- Jolly, M.R., Wen, S.W., Lapish, A., Butler, N.D., Wickins, M., Campbell, J., Investigation of running systems for gray cast iron camshafts, *Modeling of Casting, Welding and Advanced Solidification Processes VIII*, The Minerals and Metals Society, pp 67-75(1998)
- Lee, P.D., Hunt, J.D., Hydrogen Porosity in Directional Solidified Aluminum -Coper Alloys: In Situ Observation. *Acta Materialia*, Vol. 45, No.10, 1997:4155-4169
- Lee, P.D., Hunt, J.D.. Measuring the Nucleation of Hydrogen Porosity During the Solidification of Aluminum-Copper Alloys. *Scripta Materialia*, Vol. 36, No.4, 1997:399-404
- Lee, P.D., Hunt, J. D., A model of the Interaction of Porosity and the Developing Microstructure. Modeling of casting, welding, and advanced solidification processes VII. 10-15 September 1995: 585-592.
- Nguyen, T. and Carrig, J., Water analogue studies of gravity tilt casting copper alloy components, *AFS Transactions*, Vol. 94, pp 519-528 (1986)
- Perkins, N.D. and Bain, C.J., Transparent, water models as an aid to gating design for permanent mould aluminum alloy castings, *Journal of Australian Institute of Metals*, Vol. 10, No. 2, pp 160-168 (1965)
- Ruiz, D.J., Khandhia, Y. Filling and Solidification with Coupled Heat Transfer and Stress Analysis, Modeling of Casting, Welding and Advanced Solidification Processes VII, The Minerals and Materials Society, pp 991-1006 (1995)
- Rezvani, M., Yang, X., and Campbell, J., Effect of Ingate Design on Strength and Reliability of Al Castings, *AFS Transactions*, Vol107, pp181-188 (1999).
- Schuhmann, R. W., et al and Dahle, A. K., Modeling and Validation of Molten Metal Flow in Permanent Mold Casting, *AFS Transactions*, Vol 108, pp 599-607 (2000).

## 2003 Keith Millis Symposium on Ductile Cast Iron

- Stegemann, D., Reimache, W. and Schmidbauer, J., Investigation of light metal casting process by real time micro-focus radiography. *The European Journal of Non-destructive Testing*, Vol1, No.3, Jan 1992:107-117
- Sirrell, B., Campbell, J., Real-time X-ray Radiography of Mould Filling, *CASTCON '95 (Conference proceedings)*, Institute of British Foundrymen: 15-16 June 1995
- Sirrell, B., Holliday, M., Campbell, J., Benchmark testing the flow and solidification modeling of Al castings, *Journal of materials (JOM)*, Vol. 48, No. 3, pp 20-23(1996)
- Sirrell, B., Campbell, J., The effects of Mold Filtration in the Reduction of Casting Defects due to Surface Turbulence During Mold Filling, *AFS Transactions*, Vol105, pp645-654 (1997).
- St.John, Davis, D.H., K.G., Magny, J.G., Computer Modeling and Testing of Metal Flow in Gating Systems, Physical Metallurgy Research Laboratories Report MRP/PMRL 80- 12 (J), Canmet Canada Centre for Mineral and Energy Technology. (1980).
- Sun, W., Littleton, H.E., Bates, C.E., Real time X-Ray Observations on the Metal Filling of Lost Foam Aluminum Castings, *AFS Transactions*, Vol 110, pp 1347-1356 (2002).
- Xue, X., Hansen, S.F., Hansen, P.N., "Water analog study of effects of gating designs on inclusion separation and mold filling control," *AFS Transactions*, pp 199-209 (1993).
- Yang, X. Campbell, J., Liquid Metal Flow in a Pouring Basin, *International Journal of Cast Metals Research*, No. 10, pp239-253 (1998)